

Harmonic Current Reduction Method of Hand-Held Resonant Magnetic Field Charger (HH-RMFC) for Electric Vehicle

Chiuk Song, Hongseok Kim, Daniel H. Jung, Eunseok Song, Sukjin Kim, Jonghoon Kim, and Joungho Kim
 Terahertz Interconnection and Package Lab., Department of Electrical Engineering
 Korea Advanced Institute of Science and Technology
 373-1 Guseong-dong, Yuseong-gu, Daejeon, South Korea
 chiuk.song@kaist.ac.kr

Abstract— The hand-held resonant magnetic field charger (HH-RMFC) is a convenient equipment of charging the batteries without any electrical contact. Due to high coupling coefficient of HH-RMFC, the single phase power inverter with square wave encounter relatively small reactance at its harmonic frequencies. Thus, the current flowing through the Tx and Rx windings can be distorted. The distorted current with large amount of harmonics may act as magnetic near field noise to the adjacent sensitive electronic devices such as sensors, controller and communication devices in electric vehicles (EVs). Moreover, the current harmonics have the effect of increasing losses and thermal stress in power system. In this paper, a reduction method of the harmonic currents in HH-RMFC is proposed. The circuit simulation results show that the harmonic currents flowing through Tx and Rx windings in HH-RMFC can significantly be reduced by applying the proposed method. The circuit simulation results show that proposed method can reduce THD of Tx current and Rx current by 15.64 % and 14.11 %, respectively.

Keywords—Wireless power transfer, resonant magnetic field, magnetic field noise, total harmonic distortion.

I. INTRODUCTION

In the near future, electric vehicles (EVs) including hybrid electric vehicles (HEVs), plug-in hybrid electric vehicles (PHEVs), and pure battery electric vehicles (BEVs) will dominate the vehicle market. With continuously increasing EV charging station unit sale, the battery charging method is an important part to manufacturers. Among the various charging methods, the resonant magnetic field charging has advantages in terms of electrical safety and convenience. The HH-RMFC system consists of inverter, HH-RMFC, regulator and batteries. The Tx part (i.e., the primary winding) and the Rx part (i.e., the secondary winding) in HH-RMFC are combined to transfer power using magnetic field resonance. The inverter source supplies square waves, which contain a wide range of harmonics. These can generate electromagnetic radiation that interferes with the operation of adjacent sensitive electronic devices in EV. Ferrite cores are usually adapted for shielding the electrical devices from the produced magnetic field noise by guiding the magnetic field.

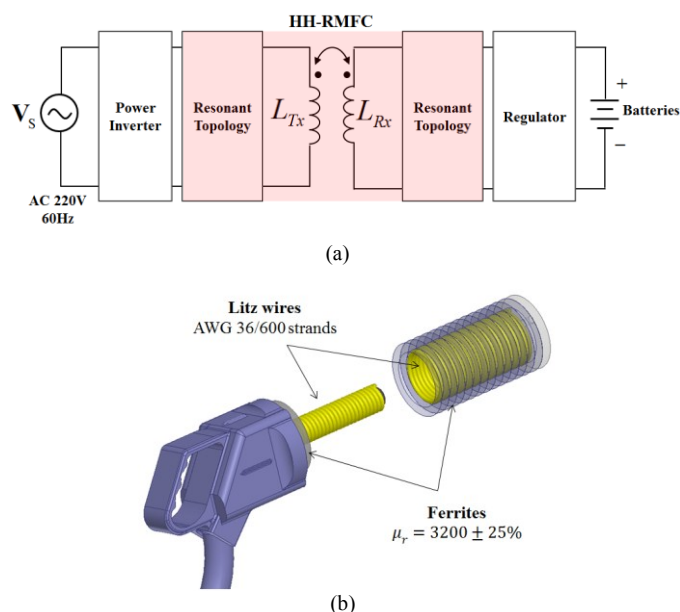


Fig. 1 (a) Simplified system block diagram of HH-RMFC system. The single phase power inverter includes AC-DC converter, DC-DC converter and DC-AC inverter; HH-RMFC includes Tx and Rx inductors for the actual wireless power transfer; the regulator includes diode rectifier and AC-DC converter; the batteries are charged by the transferred power. (b) The structure of HH-RMFC.

Besides, conductive materials can be added at the Tx and Rx parts to isolate the adjacent electric devices from EMF noise [1]. However, due to high frequency time-varying magnetic field, eddy current is induced on both shielding materials, which causes power transfer efficiency reduction and temperature rise in HH-RMFC system. Therefore, in order to reduce the effect of magnetic near field noise, harmonic current reduction is required for HH-RMFC system.

In this paper, the design method for harmonic current reduction in HH-RMFC system is proposed and verified using a circuit simulator. Total harmonic distortion (THD) is used to quantify the level of harmonics in current waveforms. In the following, an overview of HH-RMFC system, total harmonic distortion in HH-RMFC system, circuit simulation results and conclusion will be presented.

II. HANDHELD RESONANT MAGNETIC FIELD CHARGER

The 2kW-class HH-RMFC system consists of power inverter, HH-RMFC, regulator and batteries as shown in Fig. 1 (a). A high frequency operation is utilized to reduce the size and mass of the HH-RMFC. The power inverter converts the utility power (220V/60Hz) to AC power with the frequency of 20 kHz which is the authorized frequency for the wireless power transfer (WPT) application in South Korea [1]. The power is transferred from the Tx winding to the Rx winding by inducing the voltage in Rx winding by generating the magnetic flux in Tx winding. The transferred AC power is converted into DC using a rectifier for charging the batteries. The 3D FEA simulation model of HH-RMFC for electric vehicle charging is shown in Fig. 1(b). The proposed HH-RMFC is compact in size with proper ferrite thickness considering core saturation. The structure of HH-RMFC which can reduce leakage flux with closed structure has high efficiency. The model consists of a set of two magnetically coupled windings and ferrite cores. A full-bridge rectifier is selected to convert high frequency AC power into DC power with minimized ripple.

A. The Equivalent Circuit for HH-RMFC

In order to minimize the reactance of the input impedance, the resonant topology is necessary [2], [3]. Four basic resonant topologies are generally known: Series-Series (SS), Series-Parallel (SP), Parallel-Parallel (PP) and Parallel-Series (PS). Depending on the application, the advantages and disadvantages of each topology are considered. In case of battery charging in EV, the load resistance varies by the state of charge (SOC). In addition, the inductance of Tx and Rx windings depend on the temperature of ferrite. Therefore, the SS resonant topology is adapted due to the small effect of Tx capacitance variation. The capacitances in SS topology can be determined by the following equations.

$$C_{Tx} = \frac{1}{\omega_0^2 L_{Tx}} \quad (1)$$

$$C_{Rx} = \frac{1}{\omega_0^2 L_{Rx}} \quad (2)$$

The equivalent circuit for the HH-RMFC system with rectifier and regulator represented as block diagrams is shown in Fig. 2. A full-bridge rectifier is selected to convert high frequency AC power into DC power with minimized ripple. V_s and R_s are power inverter source and source resistance, respectively. L_{Tx} and L_{Rx} represent the self-inductance of Tx and Rx windings, respectively. Each resistance of Tx and Rx windings is represented by R_{Tx} and R_{Rx} , respectively. M is defined as the mutual inductance between the Tx and Rx windings. And, the capacitance for minimizing VA rating and increasing efficiency is represented by C_{Tx} and C_{Rx} . V_{FW} is the diode forward voltage. The voltage across C_{Filter} is represented by V_{avg} . I_{batt} and V_{batt} are the nominal battery charging current and the nominal battery charging voltage respectively. The nominal voltage of batteries is 72 V and the nominal charging current 28 A. The load resistance can be calculated because the required current and voltage of the battery is generally predefined. The input impedance values, R_{DC} and R_L , are given by

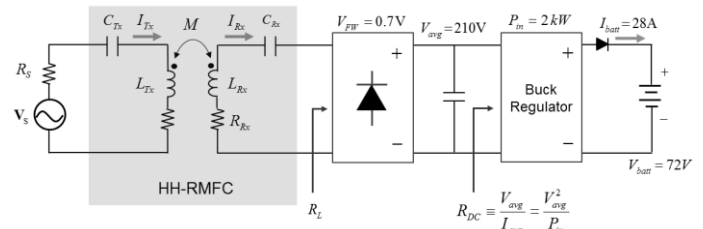


Fig. 2 Circuit representation of equivalent circuit for the HH-RMFC system with rectifier and regulator

TABLE I
ELECTRICAL CHARACTERISTICS OF HH-RMCC

Parameter	Value	Parameter	Value
L_{Tx}	179.17 μH	C_{Tx}	0.242 μF
R_{Tx}	30.35 $m\Omega$	C_{Rx}	0.378 μF
L_{Rx}	182.97 μH	R_s	1 $m\Omega$
R_{Tx}	32.63 $m\Omega$	k	0.72

$$R_{DC} = \frac{V_{avg}^2}{P_{in}} = \frac{210^2}{2kW} = 22.05 \Omega \quad (3)$$

$$R_L \approx \frac{8R_{DC}}{\pi^2} \left(1 + \frac{2 \cdot V_{FW}}{V_{avg}} \right) = 18.01 \Omega \quad (4)$$

The rest of circuital parameters of HH-RMFC for the circuit simulation are shown in Table I. The self-inductance of Tx and Rx parts are determined considering the power transfer efficiency of HH-RMFC system.

B. Total Harmonic Distortion of Current in HH-RMFC System

The output voltage waveform of the power inverter is a square wave containing many harmonics. The magnitude of current harmonics is affected by the impedance of HH-RMFC and non-linear device such as diode rectifier. Fig. 4 shows the simulation results of current flowing through the Tx and Rx windings. The current distortion in time-domain appears as current harmonics in frequency-domain as shown in Fig. 5. The current harmonics cause electromagnetic interference (EMI) and increase losses in the power system components. The distortion of current is quantified as total harmonic distortion (THD). The term expresses the distortion as a percentage of the fundamental of current waveforms. The equation for THD of current is given by

$$THD_I(\%) = \frac{\sqrt{\sum_{n=2}^{\infty} I_n^2}}{I_1} \times 100 = \frac{\sqrt{I_2^2 + I_3^2 + I_4^2 + \dots + I_n^2}}{I_1} \times 100 \quad (5)$$

where I_n is the RMS current of n th harmonic and $n = 1$ is the fundamental frequency. From (5), THD of the current flowing through Tx and Rx windings can be calculated as shown in Table I.

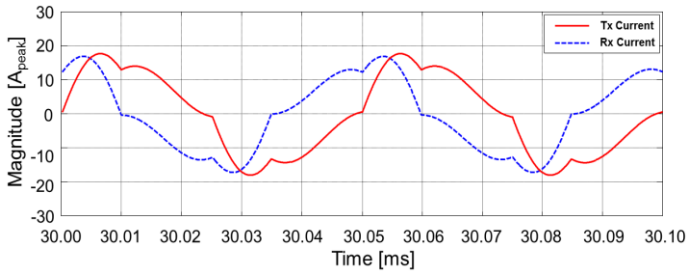


Fig. 3 Current wave forms flowing through Tx and Rx winding in time-domain without decoupled inductor

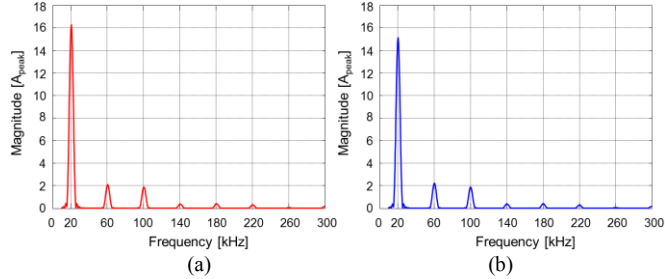


Fig. 4 (a) Frequency spectrum of Tx part, (b) Frequency spectrum of Rx part

TABLE I
THD OF CURRNT IN HH-RMFC

L_{Tx}, L_{Rx}	THD(%)	
	THD of Tx current	THD of Rx current
$50\mu H$	19.91	17.68

C. Current Harmonic Reduction Method for HH-RMFC System

To analyze the current harmonics in HH-RMFC system, a simplified equivalent circuit model with SS resonant topology is given in Fig. 5. The input impedance of HH-RMFC system is defined as

$$Z_{input} = R_s + R_{Tx} + j\omega L_{Tx} + \frac{1}{j\omega C_{Tx}} + \frac{\omega^2 M^2}{R_{Rx} + j\omega L_{Rx} + \frac{1}{j\omega C_{Rx}} + R_L} \quad (6)$$

For higher frequency, the expression for magnitude of input impedance can be rewritten as

$$|Z_{input}| \approx \sqrt{\left(R_s + R_{Tx} + \frac{\omega^2 M^2 (R_{Rx} + R_L)}{\sqrt{(R_{Rx} + R_L)^2 + (\omega L_{Rx})^2}} \right)^2 + \left(\omega L_{Tx} - \frac{\omega^3 M^2 L_{Rx}}{\sqrt{(R_{Rx} + R_L)^2 + (\omega L_{Rx})^2}} \right)^2} \quad (7)$$

The inverter voltage source supplies a square wave, which is a combination of sine waves of multiple frequencies. The magnitudes of the current harmonics are inversely proportional to the input impedance. Since the operating resonant frequency and load resistance are the design constraints, the harmonics can be reduced by increasing the inductance. However, the mutual inductance is dependent on the self-inductance of Tx and Rx parts. Therefore, in order to increase the self-inductance without increasing the mutual inductance, series decoupled inductors are added at both Tx and Rx parts as shown in Fig. 7.

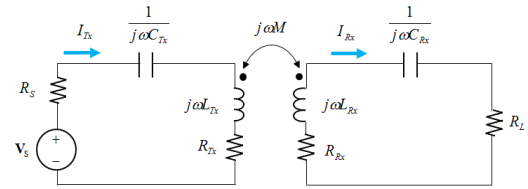


Fig. 5 Simplified equivalent circuit for the HH-RMFC system

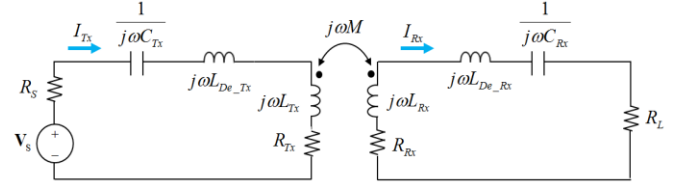


Fig. 6 The equivalent circuit with decoupled inductor for HH-RMFC

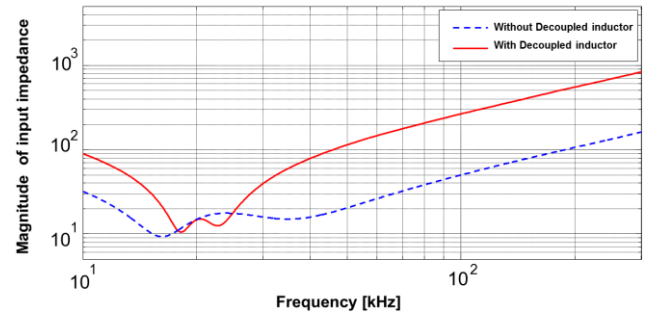


Fig. 7 Comparison of the magnitude of input impedance simulation results of HH-RMFC system with and without decoupled inductor

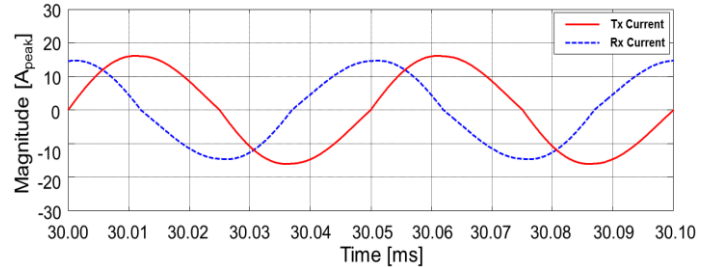


Fig. 8 Current wave forms flowing through Tx and Rx winding in time-domain with decoupled inductor

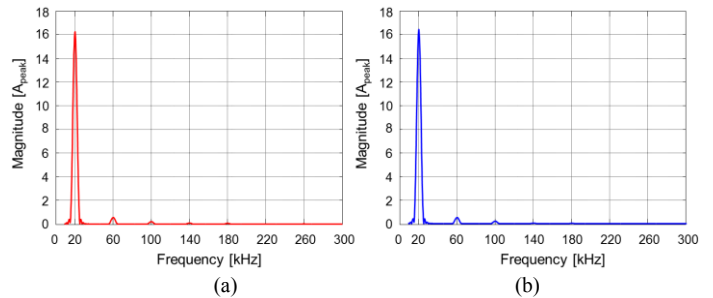


Fig. 9 (a) Frequency spectrum of Tx part, (b) Frequency spectrum of Rx part

For higher frequency, the expression for magnitude of input impedance with decoupled inductor can be rewritten as

$$|Z_{input}| \approx \sqrt{\left(R_s + R_{Tx} + \frac{\omega^3 M^2 (R_{Rx} + R_L)}{\sqrt{(R_{Rx} + R_L)^2 + (\omega(L_{Rx} + L_{De-Rx}))^2}} \right)^2 + \left(\omega(L_{Tx} + L_{De-Tx}) - \frac{\omega^3 M^2 (L_{Rx} + L_{De-Rx})}{\sqrt{(R_{Rx} + R_L)^2 + (\omega(L_{Rx} + L_{De-Rx}))^2}} \right)^2} \quad (8)$$

TABLE II
THD OF CURRNT IN HH-RMFC

L_{Tx}, L_{Rx}	THD(%)	
	THD of Tx current	THD of Rx current
50 μ H	4.27	3.57

Adding decoupled inductors increases the input impedance in higher frequency, which reduces the current harmonic components. The magnitude of input impedance curves of HH-RMFC system with and without 300 μ H decoupled inductor are compared in Fig. 7. The input impedance curve of HH-RMFC with decoupled inductor is higher than HH-RMFC without decoupled inductor in higher frequency range. Fig. 8 shows the time-domain circuit simulation results of the waveforms of current flowing through the Tx and Rx windings with decoupled inductors. Compared to the waveforms in Fig. 3, the current distortion is clearly reduced by adding the decoupled inductors. The frequency-domain of the current is shown in Fig. 9. The calculated THD with the decoupled inductors are shown in Table II. From the circuit simulation results, the current harmonics from HH-RMFC with decoupled inductor is lower than HH-RMFC without decoupled inductor.

III. CONCLUSION

The 2kW-class HH-RMFC operating at high frequency of 20 kHz for EV is simulated and analyzed. The reduction of current harmonic from HH-RMFC is required to avoid effects on other electronic devices and components in EV. In this paper, the design method for low harmonic current in HH-RMFC is proposed and verified. The circuit simulation results evidently show that the addition of decoupled inductors reduces THD of Tx current and Rx current by 15.64 % and 14.11 %, respectively.

ACKNOWLEDGMENT

This work was supported by the National Research Foundation of Korea (NRF) grant funded by the Korean government (MSIP) (No. 2010-0028680 and No. 2010-0029179).

REFERENCES

- [1] Hongseok Kim; Jonghyun Cho; Seungyoung Ahn; Jonghoon Kim; Joungho Kim, "Suppression of leakage magnetic field from a wireless power transfer system using ferrimagnetic material and metallic shielding," *Electromagnetic Compatibility (EMC), 2012 IEEE International Symposium on*, vol., no., pp.640,645, 6-10 Aug. 2012
- [2] Chwei-Sen Wang; Stielau, O.H.; Covic, G.A., "Design considerations for a contactless electric vehicle battery charger," *Industrial Electronics, IEEE Transactions on*, vol.52, no.5, pp.1308,1314, Oct. 2005
- [3] Bert Lenaerts; Robert Puers; , Omnidirectional Inductive Powering for Biomedical Implants; Katholieke Universiteit Leuven Dept. Electrical Engineering, 2009.
- [4] C. R. Paul, Introduction to Electromagnetic Compatibility, 2nd ed., Wiley Series in Microwave and Optical Engineering, Kai Chang, Ed. U.S.:Wiley-Interscience, 2006.
- [5] Guidelines for Limiting Exposure to Time-varying Electric, Magnetic, and Electromagnetic Fields (Up to 300 GHz), ICNIRP Guidelines, 1998.
- [6] Guidelines for Limiting Exposure to Time-varying Electric and Magnetic Fields (1 Hz to 100 kHz), ICNIRP Guidelines, 2010.

- [7] Seungyoung Ahn; Junso Pak; Taigon Song; Heejae Lee; Jung-Gun Byun; Deogsoo Kang; Cheol-Seung Choi; Eunjung Kim; Jiyun Ryu; Mijoo Kim; Yumin Cha; Yangbae Chun; Chun-Taek Rim; Jae-Ha Yim; Dong-Ho Cho; Joungho Kim, "Low frequency electromagnetic field reduction techniques for the On-Line Electric Vehicle (OLEV)," *Electromagnetic Compatibility (EMC), 2010 IEEE International Symposium on*, vol., no., pp.625,630, 25-30 July 2010
- [8] Chiuk Song; Hongseok Kim; Sunkyu Kong; Jung, D.H.; In-Myoung Kim; Young-II Kim; Jonghoon Kim; Joungho Kim, "Structure of handheld resonant magnetic coupling charger (HH-RMCC) for electric vehicle considering electromagnetic field," *Wireless Power Transfer (WPT), 2013 IEEE*, vol., no., pp.131,134,